Nathan Sharpes*, Dušan Vučković and Shashank Priya

Floor Tile Energy Harvester for Self-Powered Wireless Occupancy Sensing

Abstract: We investigate a concept that can reduce the overall power requirement of a smart building through improvements in the real-time control of HVAC and indoor lighting based on the building occupancy. The increased number of embedded sensors necessary to realize the smart building concept results in a complex wiring and power structure. We demonstrate a floor tile energy harvester for creating a wireless and self-powered occupancy sensor. This sensor termed as "Smart Tile Energy Production Technology (STEP Tech)" can be used to control automation in smart buildings such as lighting and climate control based upon the real-time building occupancy mapping. The sensor comprises of piezoelectric transducer, energy harvesting circuit and wireless communication. Modeling and optimization procedure for the piezoelectric cymbal transducer is described within the framework of tiles. The design and selection of a packaging technique and construction of a durable floor tile enclosure aimed at protecting the bulk piezoceramic is discussed within the constraint that the deflection of the tile should be minimal such that it is not readily perceivable by humans, thus not disturbing their gait. Experimental results demonstrate that the piezoelectric tile could provide a promising solution for wireless occupancy sensing.

Keywords: energy harvesting, occupancy sensing, piezoelectric, cymbal transducer, smart building, smart tile, STEP tech

DOI 10.1515/ehs-2014-0009

Introduction

The increasing reliance of society on technological applications within the building environment has resulted in a necessity to find methodologies for reducing overall power consumption. In this decade, energy consumption in the United States has risen to more than 93 quadrillion Btu per year, with around 41% of this energy consumption coming from buildings in the residential and commercial sectors (EIA 2011). The concept of the smart building, or a building that is aware of its occupancy and power consumption, can help in reducing the overall power draw of buildings (Nguyen and Aiello 2013). Specifically, significant improvements can be made in the highest power consuming building functions, such as HVAC and lighting, by controlling them in real-time based upon building occupancy information (Agarwal et al. 2010; Weng and Agarwal 2012). However, the increased number of sensors necessary to realize the smart building concept can also lead to extra power draw and complexity in wiring. Therefore, a self-powered occupancy sensor (one not requiring grid or battery power) would be of great benefit and major step toward realizing the smart building concept. Such a device must then power itself by deriving the energy from its environment. To fill this need, a floor tile energy harvester is proposed for the purpose of creating a wireless and self-powered occupancy sensor. This "Smart Tile Energy Production Technology (STEP Tech)" will be used to automate and control various functions in smart buildings, such as lighting and climate control, based upon the real-time building occupancy mapping. In realizing such a device, there are several challenges that need to be addressed: (i) selection of the electromechanical transducer, (ii) modeling and optimization of the electromechanical transducer, (iii) development of a packaging technique and construction of a durable floor tile enclosure that can not only protect the transducer but also the harvesting circuitry, and (iv) integration of the tile harvester with the wireless controls. In addition, there should be limited deflection of the tile to a level on the order of the deflection of shoe soles, so that the gait of the human occupants within the building is not disturbed as they walk over the tile.

In order to not disturb the motion of occupants in the building, the operation of a floor tile energy harvester should most closely mimic that of a normal floor surface in terms of appearance and mechanical stiffness. For this reason, STEP Tech tiles are designed to be placed directly below the top floor surface (e.g. carpet, laminate,

***Corresponding author: Nathan Sharpes,** Center for Energy Harvesting Materials and Systems, Virginia Tech, Blacksburg, VA, 24060, USA, E-mail: nsharpes@vt.edu
Dušan Vučković, DELTA/Technical University of Denmark, Hørsholm, 2970, Denmark, E-mail: d.vuckovic85@gmail.com
Shashank Priya, Center for Energy Harvesting Materials and Systems, Virginia Tech, Blacksburg, VA, 24060, USA, E-mail: spriya@vt.edu

decorative tile), as is illustrated in Figure 1(a), so that the floor surface appears normal. STEP Tech is also designed to fit the dimensions of standard size decorative tiles (12 in $\times$ 12 in) and be as thin as possible, so that it can be easily retrofitted into existing tile or other flooring alternatives. Additionally, STEP Tech is meant to be placed at doorways or at boundaries between rooms and building sections, so that when stepped upon, a signal is wirelessly transmitted to the centrally located smart building receiver/controller, as depicted in Figure 1(b). In this manner, real-time occupancy of individual rooms within a building can be recorded and used, for example, to turn the lights on/off (Figure 1(a)).

Mechanical stiffness of walking surfaces plays a key role in controlling many aspects of the human gait cycle, as we are very perceptive to even small changes in stiffness (or cushioning) of walking surfaces (Hennig, Valiant, and Liu 1996). Therefore, a floor tile energy harvester must feel (i.e. have similar stiffness and deflection) like a normal floor, if it is to avoid the perception of building occupants and not alter their normal gait patterns (i.e. not affect their normal behavior). If an area of the floor is perceived as different, individuals will avoid (i.e. simply step over) those areas, and thus the data on room occupancy will have inherent inaccuracy. While terrestrial locomotion of humans is capable of many different adaptations (Alexander 1991), a sudden change in ground conditions (i.e. stepping on a "soft" tile) is not desirable. This consideration is a hindrance to the energy production of the tile, as available potential energy to be harvested is in direct proportion to the tile deflection. Though, when harvesting energy from humans, consideration of human behavior is of paramount importance.

Previous efforts on floor tile energy harvesters have been left largely to the commercial sector and have relied on linear to rotation conversion mechanisms to change the vertical deflection of the tile surface into rotary motion for induction generators (Brezet et al. 2012; Kemball-Cook and Tucker 2013; Paulides et al. 2009; Seow, Chen, and Khairudin 2011). These studies have reported vertical deflections of around 10 mm that is dependent on the applied force (i.e. body weight). These relatively large deflections have been generally accepted, as the novelty and "greenness" of this technology has, thus far, outweighed the encumbrance. Allowable floor deflections are not only left to subjective human perception but also objectively defined by law (International Code Council 2011). Section 1604.3.1 of the Virginia Construction Code defines the maximum allowable deflection of floor members subject to live (i.e. human, animal) loads as $l/360$, where l is the length of the floor

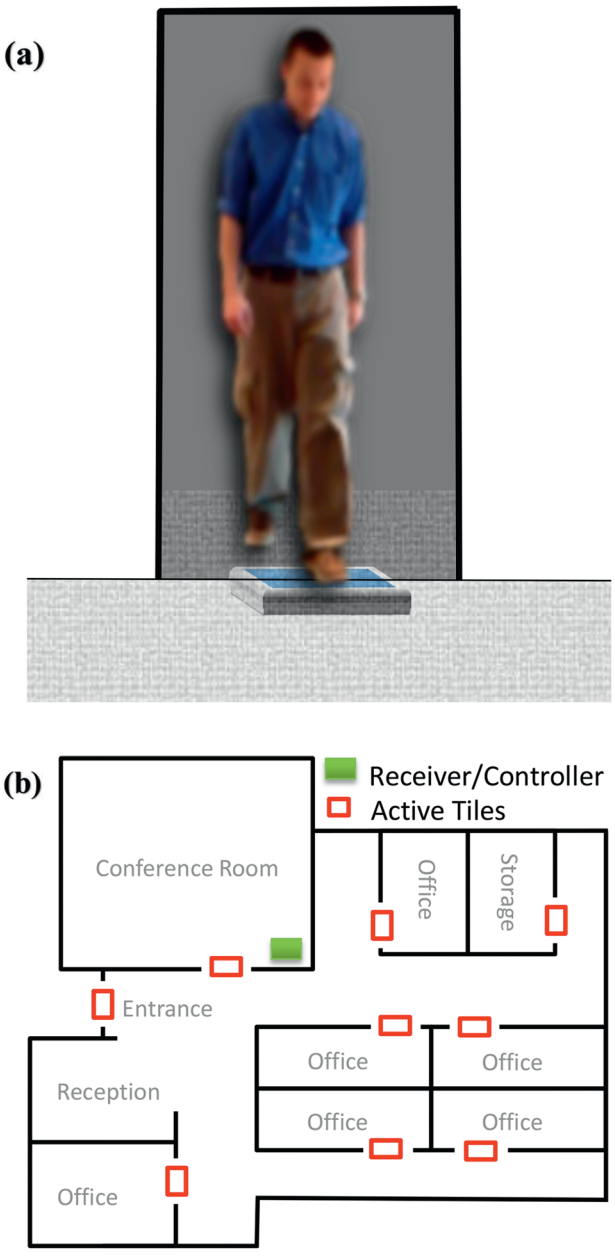

Figure 1: Illustration of (a) intended placement of individual STEP Tech tiles under floor surface in doorways and (b) distribution of STEP Tech tiles in a sample floor plan.

member. By this rule, both the Pavegen (Seow, Chen, and Khairudin 2011) (600 mm in length dimension = 1.67 mm allowable deflection) and Sustainable Dance Floor (Paulides et al. 2009) (650 mm in length dimension = 1.8 mm allowable deflection) would not be allowed to be installed in buildings in the state of Virginia, as they exceed allowable deflection limits by several times.

Since electromagnetic transducers require unacceptably large tile deflections, a piezoelectric transducer is

sought for this high-force, low-displacement application. Many shoe-mounted piezoelectrics from literature rely on forced bending to stress the piezoelectric materials (Kymissis et al. 1998). This approach is acceptable for shoes, which will last a couple of years; however, for a tile, which must last some tens of years, this technique will become less effective over time. Piezoelectrics may also be stacked in a column and compressed in the d_{33} direction (Abramovich et al. 2012). It is preferable to use piezoelectrics in the d_{33} mode, as it is typically two to three times larger than the d_{31} coefficient (APC International 2013). However, for d_{31} mode transducers, mechanical amplifiers can be used to manipulate the input forces, as exemplified in the cymbal transducer. Instead of using the cymbal shape to increase displacements as an actuator (Fernandez et al. 1998; Sun et al. 2005), it can be used to increase the force on the piezoelectric materials as an energy harvester (Kim et al. 2004; Kim, Priya, and Uchino 2006; Zhao, Yu, and Ling 2010). It has been shown that rather than using a circular cymbal, a rectangular cymbal could be used to take better advantage of the crystal orientation in the piezoelectric material (Luo et al. 2007).

The goal of this work is to demonstrate a self-powered architecture for autonomous control of the essential building functions dependent upon the occupancy. In this study, the transducer is designed based upon the rectangular cymbal configuration and will be discussed in the Modeling section with both Analytical and Finite Element Analysis models.

Modeling

Prior studies on the cymbal transducer have mostly utilized finite element simulation and experimental methods (Fernandez et al. 1998; Kim et al. 2004; Kim, Priya, and Uchino 2006; Luo et al. 2007; Sun et al. 2005; Zhao, Yu, and Ling 2010) to predict the behavior of cymbal shape. However, a simplified analytical model is lacking that can be used on a regular basis for the design and performance optimization. With an analytical model, one can easily examine the performance of different geometries in order to identify the optimum for a given set of boundary conditions. After the optimum dimensions have been identified, finite element analysis can be conducted to verify the predictions of the analytical model. This dramatically reduces the quantity of experimentation required to achieve the desired results. In this study, we follow this thought process to arrive at the optimum STEP Tech tile.

Analytical

We begin our analysis by first defining the schematic representation of the cymbal transducer, shown in Figure 2(a). The vertices of the angle bends in the end caps are labeled A-F so we may identify the individual segments of the cymbal by the lines connecting the two points. Distributed load, P, is applied to section BC, and section EF is considered to be resting on a rigid surface. Following the assumptions of Fernandez et al. (1998) that cymbal end cap bends behave as pin connected joints and the end cap members are rigid, such that there is no energy loss due to end cap bending, we add the conjecture that the bulk piezoceramic between the end caps behaves as a stiff spring. These assumptions are represented in Figure 2(b). Therefore, each cymbal section is considered to be a simple truss, and the force distribution in the structure is solved using the method of joints. Figure 2(c) shows the sign of the force in each section, with the cymbal end caps being in compression, and the piezoceramic layer being in tension. By the method of joints,

$$AB = CD = DE = AF = \frac{P}{2\sin\theta}, \quad [1]$$

and

$$BC = EF = \frac{P}{2}\cot\theta. \quad [2]$$

Therefore,

$$AD = P\cot\theta. \quad [3]$$

It is worth noting here that the cotangent of the angle θ essentially acts as an amplification factor to the applied force, P, as for any angle θ less than 45°, the $\cot\theta$ is greater than one.

With force exerted on the piezoelectric layer known, we can examine the resulting deflections of the cymbal in both the horizontal (x-axis) and vertical (y-axis) directions. The deflection in the horizontal direction is caused by the lengthening of the piezoelectric layer under tensile forces, and following our assumptions for a member with initial length, x, the deflection, dx, as shown in Figure 2(d), is equal to,

$$dx = \frac{(P\cot\theta)x}{E_pA}, \quad [4]$$

where E_p is the Young's modulus of the piezoelectric and A is the cross-sectional area of the piezoelectric layer, which for a rectangular cymbal is the thickness of piezoelectric, t_p, multiplied by its depth, b. The elongation of the piezoelectric materials in the horizontal x-direction is

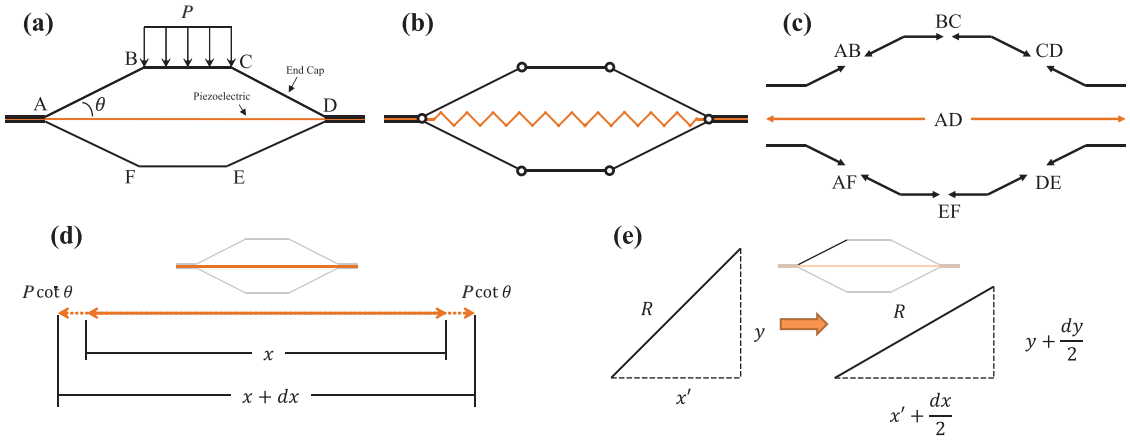

Figure 2: Schematic representations of analytical model with cymbal end caps in black and piezoelectric material in orange, and (a) diagram of cymbal with labeled points and applied force, (b) diagram with ideal model assumptions, (c) illustration of force sign in the cymbal members, (d) member responsible for horizontal (x-axis) deflection and (e) member responsible for vertical (y-axis) deflection.

accompanied by a subsequent compression of the end caps in the vertical y-direction. Examining one of the slanted segments of the cymbal end cap, such as segment AB, we see that it has some initial length, R, and rectilinear components x' and y. From our assumption of rigid cymbal end cap members, as deflection occurs, the length of segment AB remains R; however, the rectilinear components are given the addition of $dx/2$ and $dy/2$ respectively, as is presented in Figure 2(e). The deflections are halved in this case since the cymbal structure is symmetric about the center planes of the horizontal and vertical axes and we are analyzing a single end cap segment. Finally, with this information we solve for deflection in the y-direction by applying the Pythagorean Theorem to the deflected segment in Figure 2(e), where we find,

$$dy = 2\left[\sqrt{R^2 - \left(x' + \frac{dx}{2}\right)^2} - y\right]. \qquad [5]$$

Note that for this application, where the cymbal transducer is used as an energy harvester, the quantity, dy, will always be negative.

After establishing eqs [1]–[5], it becomes evident that the performance of the cymbal transducer is largely dependent on the angle, θ, which is governed by the cymbal height, h, and inner width, d_i, labeled in Figure 3(a). Using the analytical model presented thus far, the plots in Figure 3(c)-(h) are generated employing the values in Table 1, with Figure 3(b) offering a qualitative illustration of cymbal cap geometry over the parametric sweep of d_i and h. The applied load, P, for these simulations is 80 N, which is several times smaller than an average adult's weight, but was chosen because multiple cymbal transducers will be used inside the floor tile, which will distribute the applied load. The determination of the number of cymbals is described in the later sections of this paper.

From Figure 3(d) it can be seen that the largest amplification factors (the cotangent of Figure 3(c)) are observed where d_i and h become small. Naturally, as amplification factor is increased, higher force is applied to the piezoelectric layer, subsequently increasing the magnitude of displacements in both x (Figure 3(f)) and y (Figure 3(e)) directions. However, the deflection in the y-direction, which is what would be felt by the person stepping on the tile, is still significantly small, thus meeting the tile design requirements. The stress in the piezoelectric layer, plotted in Figure 3(g), is a direct result of x-direction displacement and follows the same profile as Figure 3(f). Certainly, the higher the amplifications factor, the more energy can ultimately be harvested per footstep on the tile. However, the limiting factor is the stress in the piezoelectric layer, which for the chosen material (APC 850) has a yield strength of approximately 36 MPa (APC International 2013).

In order to realize our assumption that a negligible amount of energy is lost to bending of the cymbal end caps, the end caps themselves must be as thin as possible, up to the point where they fail due to buckling, as they are under compression. The cymbal end cap members are treated as pinned-pinned plates under axial compression, as per our assumptions. The critical load for plate buckling is found using Euler's formula,

$$P_{cr} = \frac{\pi^2 EI}{L_e^2}, \qquad [6]$$

where P_{cr} represents the minimum load which can be applied to a plate before causing buckling, E the Young's

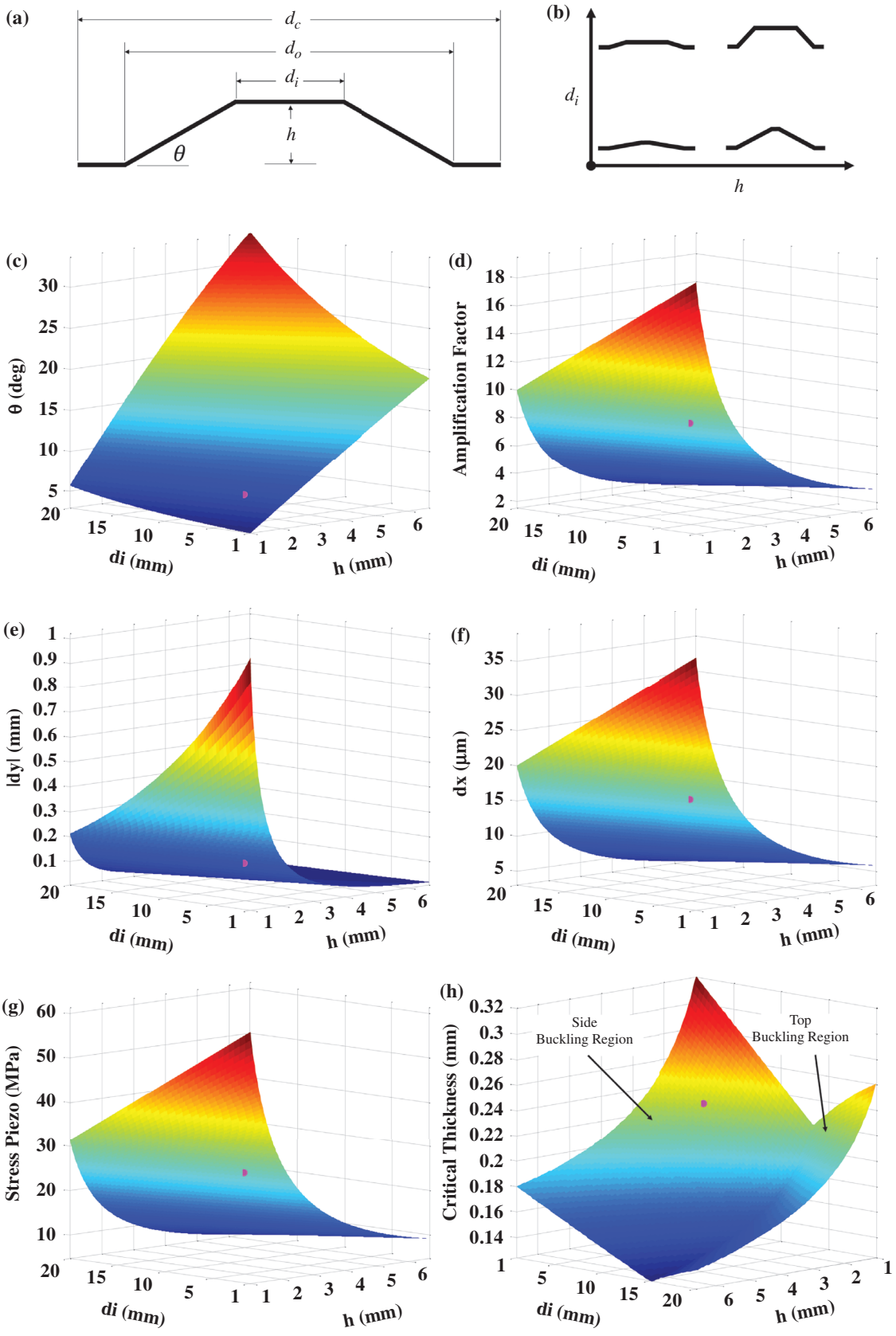

Figure 3: Results of cymbal transducer analytical modeling with (a) notation of model parameters, (b) qualitative illustration of cymbal geometry as function of parameters d_i and h. Plots (c)–(h) reveal the dependency of angle θ, amplification factor, magnitude of dy, dx, stress in the piezoelectric layer and critical thickness (to buckling) of cymbal end caps, respectively. All responses are to a static 80 N load.

Table 1: Model parameter values used for plots in Figure 3.

Parameter	Unit	Value	Description
P	N	80.0	Applied load
d_c	mm	50.0	Overall width of cymbal
d_o	mm	40.0	Width of outer cymbal bends
d_i	mm	1.0–d_o/2	Inner width of cymbal
h	mm	1.0–d_o/6	Height of cymbal cap
E_p	GPa	63.0	Young's Modulus of piezoelectric (PZT)
t_p	μm	508.0	Thickness of piezoelectric
b	mm	50.0	Overall length of cymbal
E_c	GPa	200.0	Young's Modulus of end caps (Steel)
v_c	-	0.3	Poisson Ration of end cap (Steel)
t_c	mm	0.1–1.0	Thickness of end caps

modulus of the material, I the moment of inertia and L_e the effective length (a multiple of the physical length, determined by the boundary conditions). For our case, a load is prescribed and we wish to find the necessary geometry to support that load. We then re-write eq. [6] as,

$$P = \frac{\pi^2 E_c \left(\frac{1}{12} b t_{c_{\min}}^3\right)}{\left(1 - v_c^2\right) a^2}. \quad [7]$$

where the effective length is now $\left(1 - v_c^2\right) a^2$, because we are assuming pinned-pinned joints (Rees 2009). Here v_c is the Poisson's ratio of the cymbal end cap, a is the physical length, b the width and $t_{c_{\min}}$ is the minimum end cap material thickness necessary to prevent buckling due to prescribed applied load, P. Next, eq. [7] is solved for the minimum thickness,

$$t_{c_{\min}} = \left(\frac{12P\left(1 - v_c^2\right) a^2}{\pi^2 E_c b}\right)^{\frac{1}{3}}. \quad [8]$$

The cymbal structure can experience buckling either on the slanted side sections or along the top member, depending on the relative values of d_i and h. Therefore eq. [8] makes two distinct curves as a takes the value of d_i to examine buckling in the top section and takes the value of R to examine buckling in the slanted side section. These two curves are plotted in Figure 3(h), where the greater of the two solutions is displayed for the varying geometry.

With this analysis, cymbal dimensions were chosen such that the stress in the piezoelectric layer would be approximately 75% of the yield strength, giving a Factor of Safety of 1.33, while keeping y-axis deflection at a minimum. The Factor of Safety is kept low to maximize the performance, and because the tile will be protected from overloading, as is described in a later section. Other considerations were to keep the height of the transducer small, such that the overall height of the floor tile could remain slim, making it easier to install in a floor, and keeping the inner width of the cymbal (d_i) large enough, such that the top plate of the floor tile could have a good surface to rest upon. The chosen design point is highlighted on plots of Figure 3 with a magenta marker and corresponds to $d_i = 5$ mm and $h = 2$ mm. For this geometry, the cymbal end caps would need to be at least approximately 230 μm thick. In keeping with the Factor of Safety of 1.33, the next closest available material thickness (material sold in standard thicknesses) was chosen to give t_c =305 μm.

Finite element analysis

To check the validity of the analytical model and assumptions prior to fabrication, a finite element analysis of a cymbal transducer of the dimensions chosen in the previous section was conducted. The dimensions are detailed in Figure 4(a), along with the mesh view overlaid on the cymbal transducer assembly. The material properties for the steel end caps and PZT piezoelectric layer were estimated using the available material information and were identical to that used in the analytical model, listed in Table 1. The interface of the cymbal end caps and piezoelectric layer was taken to be rigidly bonded. This analysis considers 32,115 tetrahedral elements with an equivalent 80 N distributed load applied across the top surface of the transducer and was conducted using the Stress Analysis Environment of Autodesk Inventor Professional 2013.

Examining Figure 4(b), where the coloring represents the First Principal Stress, we see that the cymbal end caps are largely in uniform compression within each segment, with only a slight amount of tensile stress on the surface by the obtuse angles due to the occurrence of some finite bending in that region. Looking at the First Principal Stress in just the piezoelectric layer, shown in Figure 4(c), we find that this layer is in uniform tension, with the exception of stress concentrations in the corners caused by material necking as it meets the bonded boundary condition. The dark colored regions on either end of the piezoelectric layer are located where the end caps are bonded and are in slight compression to support the vertical component of the reaction load applied by the end caps. Vertical (y-axis) displacement of the cymbal transducer is shown in Figure 4(d) and horizontal (x-axis) displacement is shown in Figure 4(e). Note the displacement in the horizontal direction is axisymmetric and thus the displacement, dx (elongation of the piezoelectric layer), is taken to be twice the maximum value of the Figure 4(e).

A comparison of the results from the analytical and finite element models is shown in Table 2. Here we find good agreement between the two models, with the slight

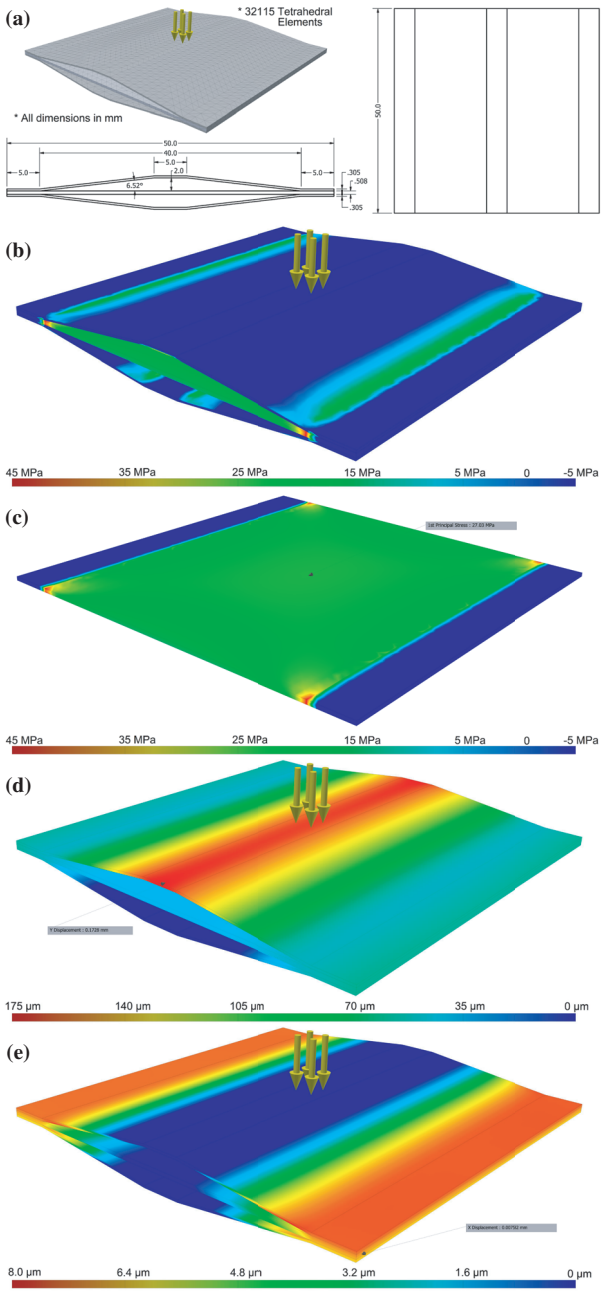

Figure 4: Results of finite element analysis of cymbal structure subject to an equivalent 80 N distributed static load across top surface using 32,115 tetrahedral elements with (a) model dimension drawings and finite element mesh, (b) first principal stress of assembly, (c) first principal stress in piezoelectric layer, (d) vertical (*y*-axis) displacement and (e) horizontal (*x*-axis) displacement.

differences being attributed to the bending of the cymbal end caps, which is neglected in the analytical model. The bending predicted by the FEA gives additional vertical displacement, *dy*, which subsequently takes away from horizontal displacement, *dx*. This energy loss is then reflected in the slightly reduced stress observed in the piezoelectric layer. The analytical model was subsequently concluded to be sufficiently accurate and a slightly conservative representation of the performance of the cymbal transducers in this specific application.

Table 2: Comparison of Analytical Model and Finite Element Analysis of the cymbal assembly of the chosen dimensions. Analytical Model shows good agreement with FEA and discrepancies are due to the small amount of bending in the cymbal caps.

Parameter	Unit	Model	FEA
dy	µm	156.6	172.8
dx	µm	17.52	15.16
Piezostress	MPa	27.6	27.03

Experimental methods

Manufacturing

The cymbal transducers deflect only a small portion of their height (around 3%) when fully compressed. For this reason, it is necessary to develop a manufacturing technique such that the dimensions of each of several cymbal transducers in the floor tile are most nearly the same. Therefore, a press-brake manufacturing technique was adopted in order to produce a consistent cymbal end cap. The press, shown on the left, and the brake, shown on the right, in Figure 5(a), were machined in a Tormach PCNC 1100 mill in a slightly exaggerated profile to allow for spring-back in the steel end caps after pressing. Flat pieces of steel shim were inserted into the press brake and bent into the desired shape, as seen in Figure 5(b). The bending pressure was applied by a hydraulic press, shown in Figure 5(c), operating at approximately 20 kpsi. Piezoelectric elements were then packaged (discussed in a later section) as shown in Figure 5(d). The elements were arranged in five parallel 60 mm by 10 mm pieces rather than one 50 mm by 50 mm piece due to material availability. The assembly was then bonded together using Loctite 120 HP epoxy, which was allowed to cure in a kiln at 65°C for no less than 12 hours. The completed assembly is shown in Figure 5(e).

Testing procedure

In order to verify the performance of the cymbal transducers in the target application, it is necessary to have the ability to impose a repeatable force input onto the system. The force applied to the ground during walking varies from person to person and even between steps

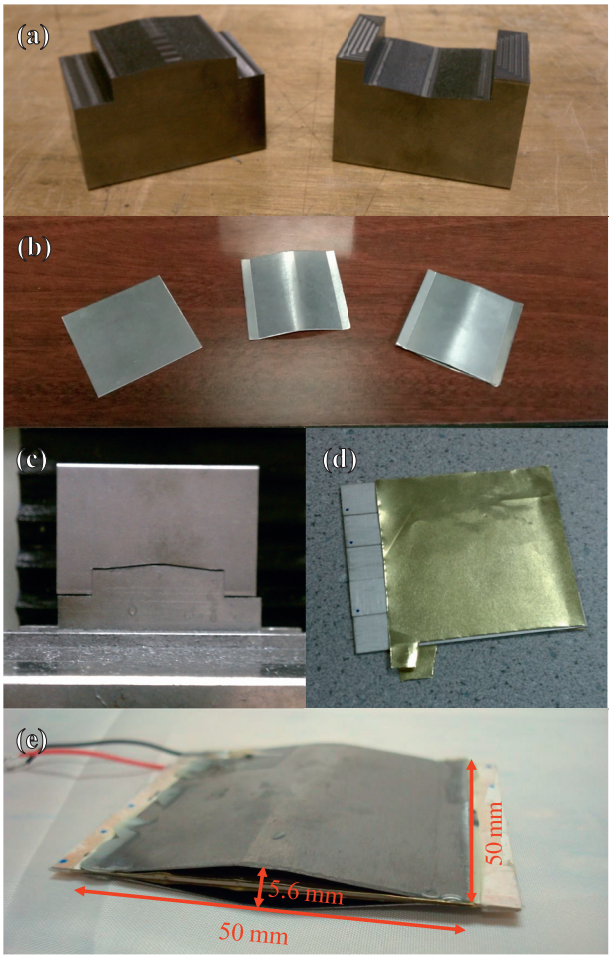

Figure 5: Manufacturing process for production of cymbal transducers whereby (a) press (left) and brake (right) are machined and used to bend (b) flat pieces of steel into shape when under pressure from (c) a hydraulic press. (d) Piezoelectric elements are then packaged and (e) the assembly is bonded together using epoxy.

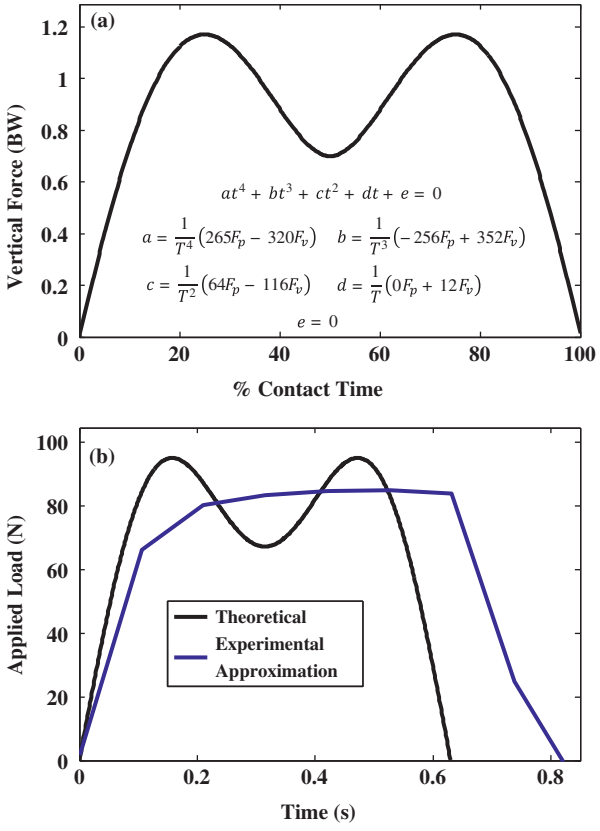

Figure 6: (a) Fourth-order polynomial curve fit of vertical ground reaction force data from Martin and Marsh (1992) and (b) typical experimental step force approximation compared to theoretical actual force profile (example for target 80 N load).

made by the same person. Thus, we first seek to find a mechanical means of applying force onto the cymbals so that the same force profile may be applied across multiple tests. This will allow for comparative analysis across a range of cymbal variables. To establish the requirements of the mechanical test stand, we first institute the force profile that needs to be simulated. In prior work, Martin and Marsh (1992) have provided the ground reaction force for persons walking at their preferred pace, from which the fourth-order polynomial curve fit in Figure 6(a) was derived. The curve was obtained under the assumption that the first peak (heel strike) occurs at 25% of the contact time, the trough (when both feet are on the ground) occurs at 50% of the contact time, and the second peak (toe-off) occurs at 75% of the contact time. The constraints were also set such that the first and second peaks were of the same approximate amplitude, which is true under steady-state walking, and the curve tends to zero at 0% and 100% contact time. With these constraints in place, the coefficients of the polynomial were solved as a function of T, the total contact time (i.e. period of the step), F_p, the peak force, and F_v the force in the valley of the curve as shown in Figure 6(a). The values of T, F_p, and F_v were chosen to be 0.63, 1.17, and 0.7, based on the findings of Martin and Marsh (1992). Note the ground reaction force (Vertical Force in Figure 6(a)) is given as a multiple of body weight (BW).

To impose the desired force profile on the transducers, the test stand shown in Figure 7(a) was constructed. The stand consists of a rigid aluminum frame, pneumatic piston, control valves, and measurement sensors. High pressure air (~110 psi building supply) was fed into the system which was then regulated to the desired pressure by either an electronic or manual pressure regulator. A three-way solenoid valve (Parker 71315SN) then applies the supply pressure to the piston or exhausts the piston pressure to the open atmosphere. Pressure inside the piston was monitored using a Wika model A-10 pressure transducer. The force exerted on the cymbal transducer

was then inferred from the piston pressure using the piston geometry. For this work, a Bimba double acting piston of 2 in diameter was used.

In practice, the force profile of Figure 6(a) is difficult to be accurately recreated using the described test rig. The difficulty arises from the limitations of various commercially available electronic pressure regulators to regulate the pressure quickly enough or without unacceptable amount of overshoot. After several trials, the electronic pressure regulator was replaced with a manual regulator, which was set at a pressure that results in the desired force amplitude. The three-way solenoid valve then creates a pseudo-square-wave of force, which was taken to be an experimental approximation, and is shown in Figure 6(b). For this approximation, inlet and exhaust pneumatic piping size was chosen such that the rising and falling slopes of the approximated force profile most closely matches the theoretical gait force profile.

In Figure 7(a), force was applied to single transducers using a hard rubber (~75 A Shore hardness) tip to evenly distribute the load. Multiple cymbals were tested using the test stand, as in Figure 7(b), by applying the load through approximately rigid acrylic plates simulating a floor tile surface. Measurements were taken using National Instruments MyDAQ and NI9229 platforms. Finally, the system was tested in a floor tile enclosure under human footstep loads, as detailed in Figure 7(c).

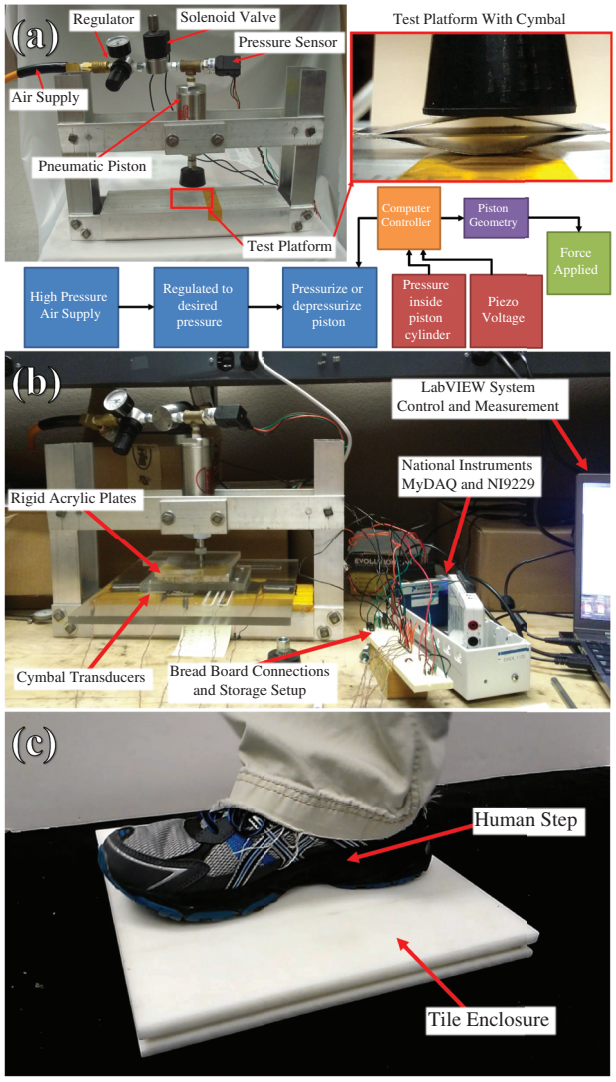

Figure 7: Experimental methods, including (a) custom test stand, illustration of flow of information and testing of single transducer, (b) multiple transducer testing using custom test stand and simulated floor tile top, and (c) testing using human step inputs.

PZT packaging

The brittle nature of lead zirconium titanate (PZT) can cause the formation of cracks over time when operating under cyclic loading conditions. Such cracks in the bulk material can reduce performance due to a complex combination of factors (Zhang and Gao 2004). This effect has been shown in practice by the East Japan Railway Company when testing their "Power-Generating Floor," where they expressed the need to package the piezoelectric elements with a protective rubber structure (East Japan Railway Company 2008). It has been shown that PZT may be made substantially more compliant by creating a macrofiber composite (Wilkie et al. 2000). It is, however, simpler and cheaper if some of the benefits realized by a fiber composite could be realized using bulk piezoelectric material. Therefore, in this study it was examined if a bulk laminate composite can be used to improve the performance of the cymbal transducer and keep the cost of ceramic at the minimal level.

To minimize the onset of brittle fracture or cracking in the PZT, it should be laminated with a more ductile material. Additionally, the laminate should have a higher Young's modulus than PZT in order to adequately transfer strain across any cracks which do form, but should be kept sufficiently thin so as to take a minimal amount of strain energy away from the PZT layer. It was thus decided to laminate the bulk PZT pieces with brass, because of its high ductility, electrical conductivity, and Young's modulus approximately 40% greater than PZT.

To examine the influence of the laminate brass layer, three cases illustrated in Figure 8(a) were considered, including a baseline case of unlamented (plain) PZT, a 25 μm brass laminate case, and a 50 μm brass laminate case. The brass was laminated at the top and bottom surfaces of the PZT using All-Spec CW2400 conductive

epoxy, bonded in a kiln at 80°C for no less than 2 hours. For these tests, smaller scale test specimens were used to minimize the material waste during ultimate breaking strength tests. The test specimens were of similar geometry to the dimensions shown in the drawing of Figure 4(a), however only 10 mm in depth. The test specimens were then tested individually using the pneumatic test stand, as shown in Figure 7(a), in terms of energy output and ultimate breaking strength. Energy output was determined by recording the voltage in a storage capacitor when the test specimen was subjected to a force impulse of 20 N load for 0.63 seconds. The storage capacitor was a 10 µF electrolytic capacitor and connected to the output from the test cymbal through a full-bridge diode (BAV21) rectifier. Energy produced was then inferred by measuring the voltage across the capacitor, by the relationship, $1/2CV^2$, where C is the capacitance and V is the voltage of the capacitor respectively. Ultimate breaking strength was determined by slowly increasing the load on the test cymbal until the moment of failure. Results are given as a percent increase or decrease over the unpackaged case, as it is a comparative analysis, and to avoid confusion with the reported performance of the full size cymbals.

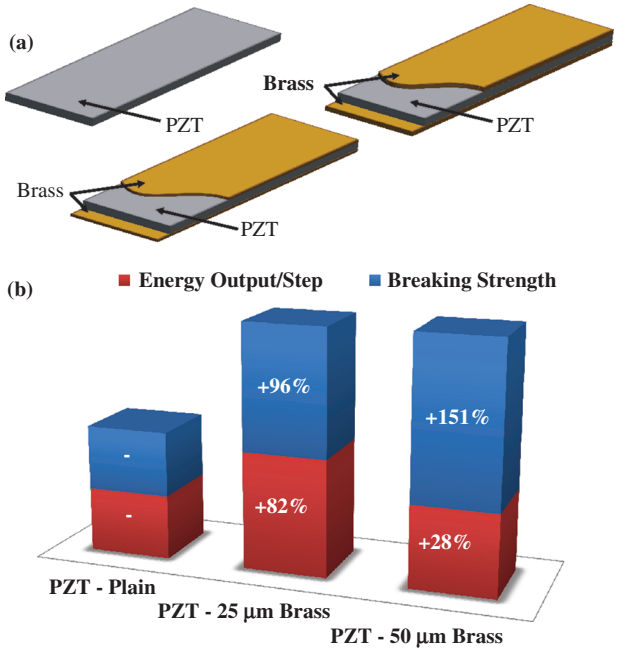

Figure 8: (a) Illustration of three packaging techniques investigated including plain PZT, PZT with 25 µm brass laminate, and PZT with 50 µm brass laminate. (b) Results of packaging test, comparing performance in terms of ultimate breaking strength and energy output per simulated step input.

As shown in Figure 8(b), the addition of the brass laminate causes a dramatic increase in breaking strength, as well as an increase in energy output per simulated step input. The increase in energy production is postulated to result from a more even stress distribution in the PZT caused by the addition of the laminate. The increase in breaking strength is more intuitively caused by the additional cross-sectional area and stiffness and subsequent reduction in stress per load. We see that while both laminate cases offer improvements in both categories, the greatest improvement, which we define as percent improvement in energy output per simulated step multiplied by percent improvement in ultimate breaking strength, is produced by the 25 µm laminate. Therefore, this packaging scheme was used for subsequent implementation in the tile.

Optimal number of transducers

We now describe the selection of optimum number of cymbal transducers that should be employed within the tile enclosure. The number of cymbal transducers determines the stress each one of them will experience and subsequently the charge produced by the PZT layer. The larger the number of transducers used, the more potential there is for energy to be harvested before the cymbals become overloaded. However, the more transducers which are used, the lower the sensitivity of the tile, or the amount of energy produced per load (i.e. person's weight). Consequently, there exists an optimum number of transducers to be employed for maximum energy harvesting from a target weight. Figure 9 illustrates this concept by showing a qualitative comparison of

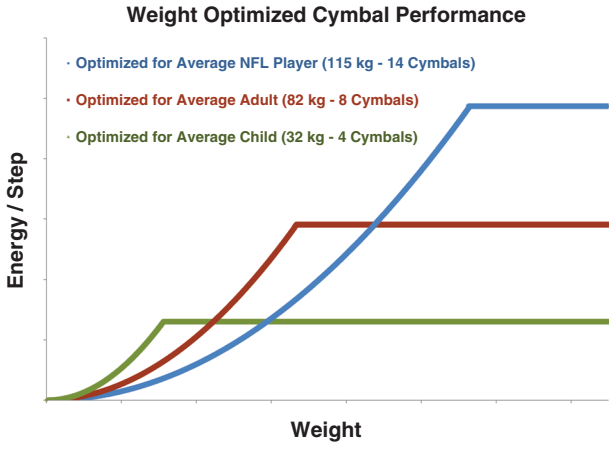

Figure 9: Qualitative illustration energy production per step as a function of weight for several cases of optimal number of cymbals used for target weights of a child (8 year old) (Fryar, Gu, and Ogden 2012), average adult (Fryar, Gu, and Ogden 2012), and average NFL player (Merron 2004) as examples.

energy produced per step on the tile, as a function of weight for an optimum number of transducers for the weight of an average child (8 year old) (Fryar, Gu, and Ogden 2012), average adult (Fryar, Gu, and Ogden 2012), and average NFL player (Merron 2004), as examples.

The flat areas of the curves in Figure 9 represent condition where the transducers would become overloaded and experience failure if not for the design of the tile enclosure (discussed in the Tile Enclosure Design section). We see that a tile optimized for a child can make much more energy per step at low weights, but has a much lower maximum possible energy production compared to a tile optimized for an adult or NFL player. We do note, however, that after a certain minimum weight, the floor tile will produce a constant amount of energy per step, regardless of the load. This type of performance is quite desirable as the function of tile (i.e. sending a signal when stepped upon) can be decoupled from a person's weight or gait style. Therefore, we determined the optimal number of transducers such that the maximum possible energy harvested per step is just sufficient to power the signal transmission circuitry. For any person above a certain minimum weight, the tile will function in a similar manner. For reasons discussed in the Circuit Design section, this minimum weight was found to be around 36 kg and an optimal number of cymbal transducers was found to be five. In this application, a minimum necessary number of transducers were used. However, if the tile was built to harvest as much energy as possible, the number of cymbal transducers would be chosen to correlate with the expected average weight of occupants that would step on the tiles most regularly.

Tile enclosure design

The main functions of the tile enclosure are to provide a flat and rigid surface to transfer force to the cymbal transducers, protect the cymbals from overstraining, and protect the cymbals and circuitry components from the environment. To ensure a consistently flat and sufficiently rigid surface, it was chosen to construct the tile enclosure from Delrin®, a thermoplastic which exhibits high stiffness, dimensional stability, low thermal expansion, and resistance to water and other chemicals. Channels were cut (CNC Mill) into the top and bottom plates, into which the supports are fitted. The support strips were bonded only to the bottom plate, using Loctite 120 HP epoxy, and were sized such that they do not come into contact with the top plate when the tile is not loaded and the top plate rests on the cymbal transducers. In Figure 10(a), we can see that when the tile is loaded, the cymbal transducers are compressed, although before the piezoelectric layer is strained to the point of failure, the top plate comes in contact with the supports, preventing further deflection. In this way, the cymbal transducers are protected from failure due to high loads. In addition, after a certain minimum load (i.e. person's weight), energy production is held relatively constant, as the deflection of the cymbal transducers is mechanically limited. This leads to a more

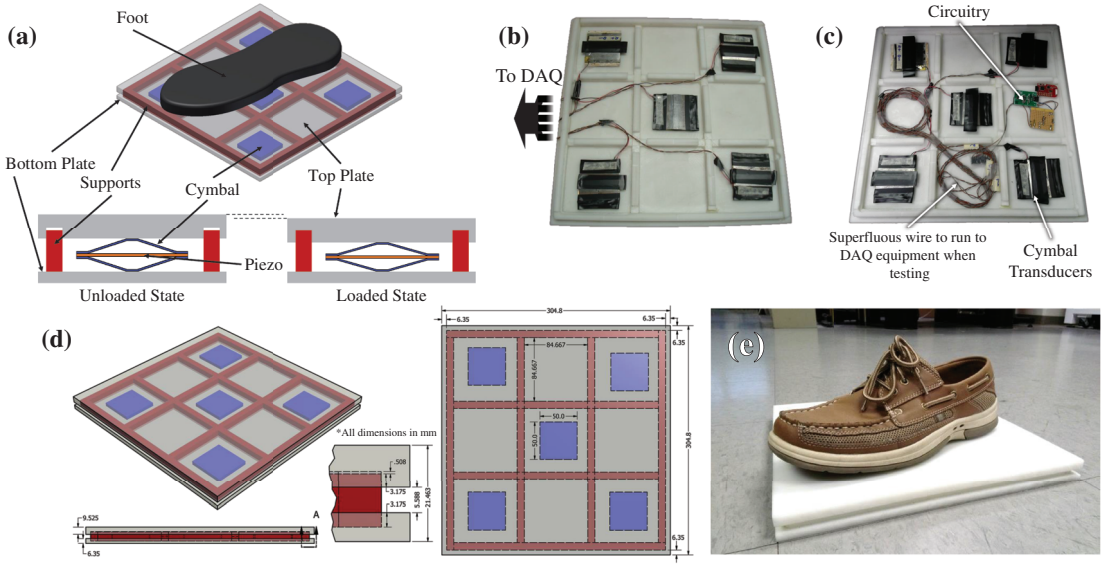

Figure 10: (a) Illustration of tile enclosure parts in unloaded and loaded states, (b) fabricated enclosure (with top plate removed) used when testing with human step inputs, (c) final fabricated enclosure (with top plate removed) with all components internal to the tile, (d) dimensioned drawing of floor tile enclosure, and (e) fully assembled STEP Tech floor tile with size 9 (US) shoe for scale.

consistent operation (i.e. occupancy sensing and signal transmission), as a known amount of energy is delivered to the circuitry.

When developing the cymbal transducers and circuitry with human step loading, as shown in Figure 7(c), the output from the cymbal transducers was run outside the tile enclosure to the data acquisition (DAQ) modules, as shown in Figure 10(b), through small holes in the enclosure, which were later filled. Once the system was verified to function as anticipated, the circuitry was wired into the enclosure and superfluous wire which was used to reach the DAQ equipment in Figure 10(b) was wound in the extra space within the tile as shown in Figure 10(c). A dimensioned drawing of the tile enclosure is shown in Figure 10 (d) with the fully assembled STEP Tech floor tile shown in Figure 10(e), along with a size 9 (US) shoe for scale.

Circuit design

With the mechanics of the tile established, circuitry was designed to fulfil the target application of detection of building occupancy. The detection of human presence was achieved by transmitting a wireless signal using the energy generated by a person stepping on the tile. In this way, each time a signal was received from the tile, it would indicate that a person has stepped on it. In order to achieve this functionality, the design was examined into four stages: (i) determining the optimal electrical connection strategy for the multiple cymbals, in order to maximize the collected energy; (ii) determining a rectification method; (iii) sizing the storage capacitor; and (iv) utilizing the collected energy through an energy management section in order to power a wireless transmitter. Each of these stages will be addressed in more detail in the following sub-sections.

Electrical connection strategy

While the cymbal transducers are loaded mechanically in parallel, their electrical connection strategy must be decided in order to realize the most efficient operation of the circuitry. When a 71 kg person stepped on the tile, it was seen that the output open circuit voltage of the cymbals is in range of 20 V to 30 V. Therefore, it can be expected that the maximum power point (MPP) will be one half of the open circuit voltage. If we consider connecting the cymbals in series, this would yield the maximum power point voltage of approximately 75 V in the case of a tile with 5 cymbals. This was derived under the assumption that all cymbals were the same, and that their maximum power point voltage was 15 V for each cymbal. In this case, the energy management stage would be faced with the task of converting the 75 V stored on the capacitor to 3 V, which is the voltage typically used by sensors and wireless modules. After searching for high efficiency DC/DC converters with the required input voltage rating, it was concluded that the conversion from 75 V to 3 V would be very inefficient. Furthermore, integrated solutions for low power switching DC/DC converters capable of performing the task are not easily available. Therefore, connecting the cymbals in series was not an option. On the other hand, connecting the cymbals in parallel would result in approximately 15 V maximum power point. At this voltage level, it was possible to use off-the-shelf converters, while providing high efficiency in energy transfer from the buffer capacitor to the rest of the circuitry. It was therefore decided to connect the cymbals electrically in parallel.

Rectification of the AC signal

In the literature, several different approaches have been demonstrated for piezoelectric output rectification (Beeby and White 2010; Erturk and Inman 2011; Guyomar et al. 2005). These circuits have been primarily designed to operate with stable periodic oscillations that would generate a predictable output of the harvester. However, the output of the cymbals when stepped on is an irregularly shaped single pulse. Furthermore, the amount of available energy after one step is in order of one millijoule. Hence, the rectification circuit selected has to be very efficient in order to not consume more energy than the gain of using the selected rectifier circuit. Furthermore, the storage capacitor can be considered empty before each step occurs, as an indeterminate amount of time will pass between the subsequent foot falls on the tile. Advanced rectifier designs typically require stable power for the control circuitry. All these limitations made the use of the advanced rectification a very challenging task. Therefore, a standard diode bridge was selected.

Selection of a storage capacitor

As with many energy harvesting applications, in this specific tile application there is not sufficient instantaneous energy produced to power the payload device (wireless signal transmitter in this case) continuously. Therefore, an intermittent storage capacitor is necessary to accumulate energy until signal transmission can be

powered. Here, there is no need for accumulating energy between transmissions, principally because occupancy has already been counted, and also because energy is only collected when the tile is being stepped upon. Therefore, the capacitor buffer size was selected based on the value that would produce the most optimal energy output from a single step. Empirically, the value of the buffer capacitor was selected to be a 10 µF ceramic X7R capacitor rated for 25 V, as it stores the most energy per step, demonstrated in Figure 11. Note that in Figure 11 one simulated step input was signified by two rises in capacitor voltage, where one rise is caused by force being applied and the second rise by the force being removed. The regions of decreasing voltage in-between rises are caused by the high leakage current of the Schottky diodes used in the full bridge rectifier above 15 V. Schottky diodes are thus not used in the final circuit design.

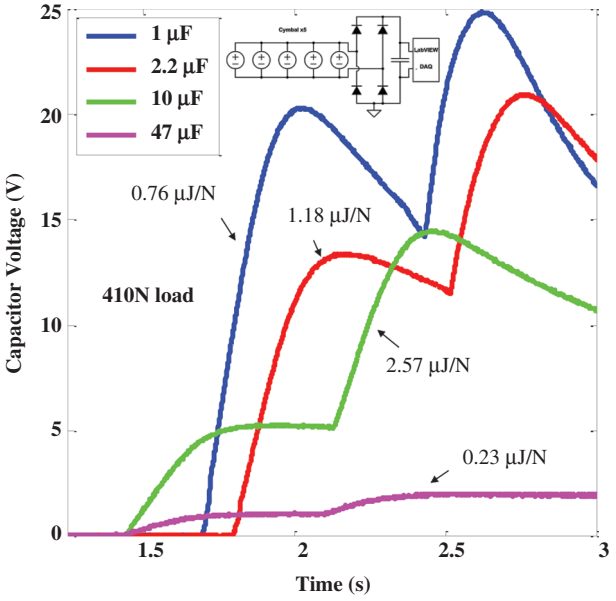

Figure 11: Stored voltage for five cymbal transducers in parallel under 410 N simulated step for varying storage capacitor values. Values of maximum energy stored per step per cymbal per load are noted for each capacitance value.

Energy management

Wireless signal transmission was performed using the ez460-RF2500 platform by Texas Instruments (Texas Instruments 2009). The energy required for starting up the transmitter and performing a wireless transmission, based on the documentation provided by Texas Instruments, was approximately 100 µJ (Morales and Shivers 2007). The amount of energy harvested during the stepping onto the tile, by an approximately 71 kg person, was borderline sufficient to perform the transmission. This, however, indicates that a lighter person wouldn't generate sufficient energy, by stepping onto the tile, to perform a transmission. In order to address this issue transmission was delayed until the person steps off the tile. A similar amount of energy is generated as a person steps off the tile as when stepping on. Therefore, as is addressed in the Optimal Number of Transducers section, the minimum weight of a person necessary to power signal transmission is around 36 kg. Based on the measurements, when the stepping off is completed, the voltage reached values around 15 V. As a result, it was necessary to convert the voltage on the storage capacitor to the range of 1.8 V to 3.6 V, which is required for stable operation of the radio and MCU on the ez430-RF2500 board. The conversion is done by using a switching DC/DC regulator. Such a regulator is found in the LTC3129-1 nanowatt buck-boost DC/DC (Linear Technology Corporation 2013). This DC/DC converter was selected first because the circuit is rated for the voltage range expected on the buffer capacitor, and second it has analog control, which can be used for selecting a threshold voltage at which the converter should activate. By applying a voltage level above 1.22 V on the analog control pin, the converter would activate. Therefore, by providing the voltage from the input using a simple resistor divider it was possible to set the activation voltage at a desired input storage capacitor voltage level. However, this circuit has a narrow input hysteresis, so it is necessary to extend it in order to allow the output to use as much energy as possible before the DC/DC converter turns off. The hysteresis extension is implemented by connecting a diode and a capacitor to the RUN input, which controls the converter's operation, as shown in Figure 12(a).

The circuit rectifies alternating voltage input from the cymbal transducers during a step. As the voltage on the input capacitor, C8, rises, the voltage on the capacitor connected to the RUN pin, C7, also rises, at a rate defined by the voltage divider and the diode voltage drop. When the voltage on capacitor C7 reaches the threshold voltage of the converter, 1.22 V, the converter starts operation. As soon as the converter starts operating, the voltage on capacitor C8 will drop, as the harvester is not capable of supplying sufficient power to prevent this, as the footstep on the tile is completed. With the drop of voltage on C8, if it weren't for the diode D5, the voltage on the RUN pin would reflect the voltage change on the input, leading to disabling the converter once the voltage on this pin reaches 1.11 V. However, as the diode is preventing the discharge of the capacitor C7, the LTC3129-1 continues operation, draining the input capacitor until it reaches 1.9 V, where the LTC3129-1 enters under-voltage condition

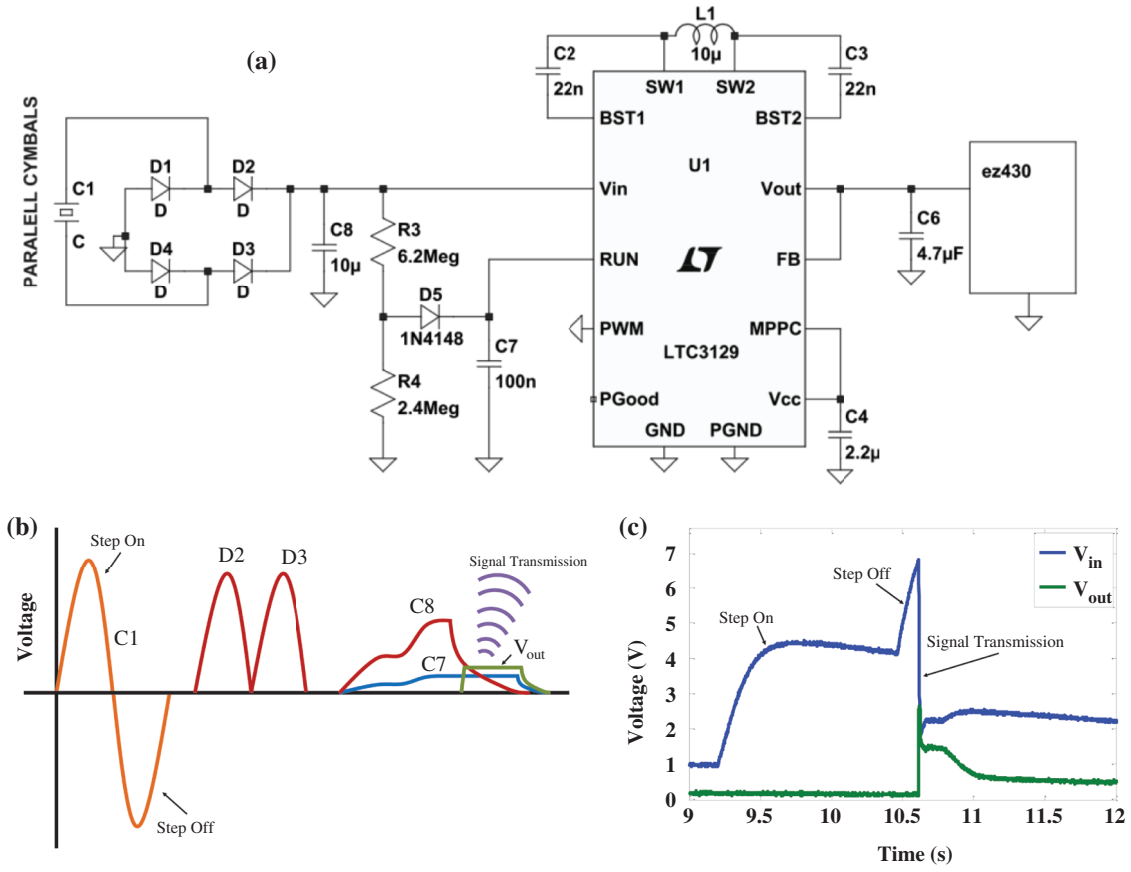

Figure 12: (a) STEP Tech circuitry schematic, with (b) qualitative illustration of circuit function, and (c) measured voltage response of circuit to simulated footstep forcing input to the tile.

and stops powering the output. This process is qualitatively illustrated in Figure 12(b), with measured voltages on the input and output sides of the DC/DC converter under simulated stepping loads shown in Figure 12(c).

Introduction of the diode D5 and the capacitor C7 to the circuitry has the effect of realizing a low pass filter on the RUN pin. This in turn introduces a delay in response to the changing input. The value of the resistance divider is in megaohm range, in order to reduce the losses during charging. Therefore, the time constant of the RC network would be in the second range, depending on the values of the resistors and capacitor used. This delay could be potentially used to the advantage of the circuit. Let VTHR-DC/DC be the voltage level required for the input storage capacitor to reach in order to provide sufficient energy to perform a wireless transmission. This voltage level will be reached, as explained earlier, during the stepping off from the tile. If a person's weight is the same as the minimum weight required for the system to operate, after the person has stepped off, the buffer would reach the required voltage VTHR-DC/DC after the delay introduced by the RC circuit. However, if a person is heavier, the voltage on the input buffer capacitor would continue to rise as the circuit is not being activated because of the said delay. In this way, more energy will be accumulated in the storage capacitor before the circuit is activated, hence providing additional energy to the circuit, increasing robustness.

Discussion

STEP Tech was tested in a "real world" setting at the Change the World Science & Engineering Careers Fair at Dulles Town Center in Dulles, Virginia. The event was attended by several hundred individuals, and the STEP Tech tile was stepped upon many times, by persons weighing an estimated range of 25–130 kg. The demonstration showed the ability of the STEP Tech tile to harvest enough energy from a single step to transmit a wireless signal to a lamp which turned on when tile is stepped upon, and turned off when the tile was stepped upon again. A sample demonstration is shown in several frames in Figure 13. From this demonstration it was

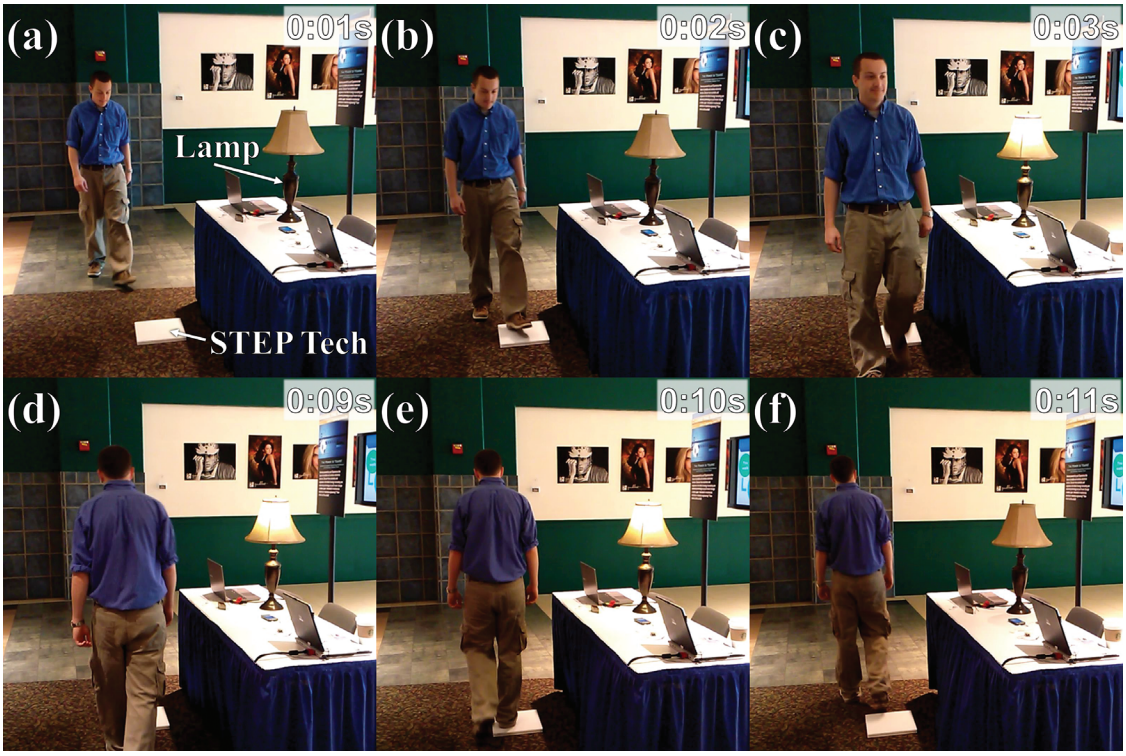

Figure 13: Lighting control demonstration whereby (a) a STEP Tech tile is placed some distance away from a lamp and when (b) the tile is stepped upon, enough energy is collected to (c) transmit a signal to the lamp to turn on. When the tile is stepped upon once again (e), the same process occurs only this time (f) turning the lamp off.

conceptualized how a distributed network of tiles could control not only smart building lighting but also climate control and other systems, based on real-time occupancy measurements. Additionally, the individuals stepping on the tile unanimously stated that they could not perceive any vertical deflection of the tile's top plate while stepping upon it. This response indicates that if the tile were embedded into a floor, it would be unperceivable to building occupants and thus not alter their normal gait patterns.

The vertical deflection of the tile is unperceivable by humans because it is mechanically limited to approximately 0.5 mm. By Section 1604.3.1 of the Virginia Construction Code, STEP Tech tiles would be allowed to deflect 0.85 mm (International Code Council 2011). Therefore, the installation of STEP Tech tiles would be allowed in buildings in the state of Virginia, unlike other commercially available floor tile energy harvesters, which report an order of magnitude greater deflection (Paulides et al. 2009; Seow, Chen, and Khairudin 2011). In addition, the level of deflection exhibited by STEP Tech tiles is not readily perceivable by persons stepping on the tile. Subsequently, STEP Tech will not disturb the gait of smart building occupants when imbedded under the floor surface (e.g. carpet, laminate, decretive tile), and thus not cause them to deviate from their normal route (i.e. avoid "soft" tiles). This then allows for accurate real-time occupancy mapping and occupancy driven smart building system control, which will lead to substantial energy savings (Agarwal et al. 2010; Nguyen and Aiello 2013; Weng and Agarwal 2012). Most importantly, these savings are realized without using sensors which consume power themselves, as STEP Tech derives its energy from human motion.

The sensors currently used in the buildings are mainly motion detectors which emit radiation into a space and detect occupancy by measuring what is reflected back to the device. Infrared sensors can also be used to detect motion through a plane. Since the premise of operation of these sensors requires that they emit energy, their power consumption is in the range of hundreds of milliwatts to several watts, depending on the device range and coverage area (Leviton Manufacturing Co. 2011). Since these devices are constantly scanning their environment, this power consumption is persistent 24 hours a day, regardless of building occupancy. Certainly, if a room containing several hundred watts of lighting can be controlled with a one watt sensor, the advantages are obvious. However, the elimination of passive energy consumption of traditional occupancy sensors, offered by an energy harvesting solution like STEP

Tech, is favorable. Naturally, the receiver for the control unit has some power consumption, but since it only needs to listen for a signal (rather than broadcast and receive), the control unit operates nearly exclusively in stand-by mode, consuming only some microwatts of power.

In addition, the control of building function through traditional occupancy sensors has proven inadequate, requiring sophisticated data analysis and redundant sensor measurements to achieve a higher certainty of occupancy detection (Dodier et al. 2006). Consequently, occupancy measurements are often left under-sampled, and rely on sensor timeouts to decide when to turn lights off, as anyone who has ever had to get up and wave their arms around to turn the lights back on in a motion detector driven lighting controlled room has experienced. STEP Tech offers the additional information about the number of people in a given area, as a signal is sent each time there is a footfall onto the tile, unlike traditional motion detectors which only see there is some level of motion in an area. Furthermore, STEP Tech tile could be arranged to capture successive footfalls, giving information about the direction of occupant motion.

Since the $Pb(Zr,Ti)O_3$ composition was discovered in the mid 1950s, many studies on developing high performance piezoelectric materials have been conducted. The commercialized piezoelectric ceramic compositions with high d_{33} value of 1,000 pC/N or compositions with high g_{33} value of 40×10^{-3} V m N^{-1} can be found. However, compositions having high d_{33} usually show low g_{33} value while high g_{33} compositions possess low d_{33}. Thus, the achievement of high $d{\cdot}g$ coefficient from single piezoelectric composition is challenging. Recently, a very different strategy for overcoming the fundamental limitations imposed by electrodynamics and thermodynamics has been proposed via designing a textured microstructure, which can result in large magnitude of $d{\cdot}g$ coefficient (Yan, Wang, and Priya 2012). The reason for realizing high $d{\cdot}g$ coefficient in textured ceramics is: (1) <001> texturing (grain orientation along the <001> crystallographic direction) of piezoelectric ceramic produces engineered domain state similar to that of <001> single crystals, thus, resulting in high d values; (2) the existence of low ε templates produces a composite microstructure and suppresses the dielectric constant (ε) of piezoelectric ceramic. Thus, utilizing textured ceramics within the cymbal transducer would result in some improvement of the output power response.

Apart from the piezoelectric materials, the power density of STEP Tech could be improved by further examination of the cymbal transducer. In this study, the end caps of the cymbal were made as thin as possible to minimize energy loss in bending the end caps and maximize the stress delivered to the piezoelectric layer. Cymbal dimensions, particularly the bend angle, were then chosen to fulfill a prerequisite Factor of Safety. Since the amplification factor of the cymbal transducer follows the cotangent of the bend angle, further decreasing the bend is predicted to increase performance. However, it is difficult to produce a cymbal end cap with angles smaller than those described in this work. This is because the bends become less sharp with decreasing angle, as plastic deformation in the pressing process is not readily induced, because of the smaller applied strain. Subsequently, buckling of the end caps becomes more spontaneous, due to the imperfect small angle bends. It is postulated that the end caps could be made slightly thicker, allowing for smaller angles to be created while still guarding against buckling. Therefore, while some performance is lost by using thicker end caps, the performance gain for using smaller bend angles would still yield an overall increase in performance.

Outside the engineering challenges, occupancy sensors in general face challenges with acceptance, as it is difficult to accurately predict cost savings (Von Neida, Manicria, and Tweed 2001). It is well established that cost savings are to be had by implementing occupancy sensors; however, as savings are ultimately directed by building occupancy and human tendency, they are inherently highly variant. In addition, there is also the consideration that frequent switching of lighting on/off can decrease light fixture lifetime, due to more rapid thermal cycling. In the case of fluorescent lights, it has been simulated that the calendar life of lighting (i.e. time between when lighting is replaced/required maintenance) may be decreased by frequent switching; however, cost savings will nonetheless still be realized (Maniccia et al. 2001). The greatest energy (and subsequently cost) savings are ultimately determined by what is done with the building occupancy information. STEP Tech offers a more reliable method of measuring occupancy without having any passive power consumption, as well as, offering savings in simplified installation and wiring costs when compared to traditional means of occupancy sensing.

Summary

In this study, a self-powered wireless occupancy sensor has been designed in order to take a major step toward practicalizing the smart building concept. Our device takes the form of a floor tile, which powers the wireless

signal transmission of occupancy information by deriving energy from human gait when stepped upon. This Smart Tile Energy Production Technology (STEP Tech) has demonstrated the ability to control automated process in smart buildings, in this case lighting, and can be easily extended to climate control and many other electronically controlled building systems. In realizing STEP Tech, several major challenges were addressed, including the modeling and optimization of a rectangular cymbal piezoelectric transducer, the development of a packaging technique and construction of a durable floor tile enclosure aimed at protecting and prolonging the useable life of the piezoceramic, as well as, the design of energy harvesting circuitry for optimal energy conversion and wireless signal transmission, and finally experimentation and demonstration to prove "real-world" functionality. These accomplishments were made while also limiting the deflection of the tile to an unperceivable level, so the gait of the building occupants is not disturbed as they walk about, preserving the integrity of the measured occupancy.

Acknowledgments: The authors would also like to acknowledge the contributions of: Jeffery Cotter (Undergraduate researcher at Virginia Tech, Blacksburg, VA) and Rob Culbertson (US Army Veteran) (Teacher at Thomas Jefferson High School for Science & Technology, Alexandria, VA).

Research funding: This research was supported through the National Science Foundation through CEHMS and Fundamental Research Program. Piezoelectric materials were donated by American Piezo Ceramics Inc. (Mackeyville, PA).

References

Abramovich, H., C. Milgrom, E. Harash, L. E. Azulay, and U. Amit. 2012. "Multi-layer Piezoelectric Generator." US8278800 B2.

Agarwal, Y., B. Balaji, R. Gupta, J. Lyles, M. Wei, and T. Weng. 2010. "Occupancy-Driven Energy Management for Smart Building Automation." In *Proceedings of the 2nd ACM Workshop on Embedded Sensing Systems for Energy-Efficiency in Building*.

Alexander, R. M. 1991. "Energy-Saving Mechanisms in Walking and Running." *Journal of Experimental Biology* 160(1):55–69.

APC International, L. 2013. "Physical and Piezoelectric Properties of APC Materials". Accessed February 27, 2014. https://www.americanpiezo.com/images/stories/content_images/pdf/apc_materials_properties.pdf

Beeby, S., and N. M. White. 2010. *Energy Harvesting for Autonomous Systems*. 685 Canton Street Norwood, MA 02062: Artech House.

Brezet, J. C., A. J. van Doorn, S. van Dongen, A. Randag, A. J. Jansen, J. J. H. Paulides, and E. A. Lomonova. 2012. "Floor Suitable for Generating, Converting and/or Storing Energy." US8283794 B2.

Dodier, R. H., G. P. Henze, D. K. Tiller, and X. Guo. 2006. "Building Occupancy Detection Through Sensor Belief Networks." *Energy and Buildings* 38(9):1033–43.

East Japan Railway Company. 2008. *Demonstration Experiment of the "Power-Generating Floor" at Tokyo Station*, 3. Retrieved from http://www.jreast.co.jp/e/development/press/20080111.pdf, January 23rd, 2013.

EIA, U. 2011. "Annual Energy Review". *Energy Information Administration, US Department of Energy: Washington, DC*. Accessed February 11, 2014. http://www.eia.doe.gov/emeu/aer

Erturk, A., and D. J. Inman. 2011. *Piezoelectric Energy Harvesting*. The Atrium Southern Gate, Chichester West Sussex PO19 8SQ England: John Wiley & Sons.

Fernandez, J., A. Dogan, J. Fielding, K. Uchino, and R. Newnham. 1998. "Tailoring the Performance of Ceramic-Metal Piezocomposite Actuators, 'Cymbals'." *Sensors and Actuators A: Physical* 65(2):228–37.

Fryar, C. D., Q. Gu, and C. L. Ogden. 2012. "Anthropometric Reference Data for Children and Adults: United States, 2007–2010". *National Center for Health Statistics*." *Vital Health Stat* 11(252):1–40.

Guyomar, D., A. Badel, E. Lefeuvre, and C. Richard. 2005. "Toward Energy Harvesting Using Active Materials and Conversion Improvement by Nonlinear Processing." *Ultrasonics, Ferroelectrics and Frequency Control, IEEE Transactions on* 52(4):584–95.

Hennig, E. M., G. A. Valiant, and Q. Liu. 1996. "Biomechanical Variables and the Perception of Cushioning for Running in Various Types of Footwear." *Journal of Applied Biomechanics* 12:2).

International Code Council, I. 2011. "Structural Design." In *2009 Virginia Construction Code*, 64. 4051 West Flossmoor Road, Country Club Hills, IL 60478.

Kemball-Cook, L., and P. Tucker. 2013. "Energy Harvesting." US20130068047 A1.

Kim, H. W., A. Batra, S. Priya, K. Uchino, D. Markley, R. E. Newnham, and H. F. Hofmann. 2004. "Energy Harvesting Using a Piezoelectric "Cymbal" Transducer in Dynamic Environment." *Japanese Journal of Applied Physics* 43(9R):6178.

Kim, H. W., S. Priya, and K. Uchino. 2006. "Modeling of Piezoelectric Energy Harvesting Using Cymbal Transducers." *Japanese Journal of Applied Physics* 45(7R):5836.

Kymissis, J., C. Kendall, J. Paradiso, and N. Gershenfeld. 1998. "Parasitic Power Harvesting in Shoes." *Wearable Computers, 1998. Digest of Papers. Second International Symposium on*.

Leviton Manufacturing Co., I. 2011. "Occupancy Sensor Applications Guide". Accessed January 28, 2013. Retrieved from: http://www.leviton.com/OA_HTML/ibcGetAttachment.jsp?cItemId=ILChMKVMbpuBNd6s8oLWow

Linear Technology Corporation. 2013. "LTC3129-1, 15V, 200 mA Synchronous Buck-Boost DC/DC Converter with 1.3 μA Quiescent Current". Accessed June 4, 2014. http://cds.linear.com/docs/en/datasheet/31291fa.pdf

Luo, L., Y. Tang, F. Wang, C. He, and H. Luo. 2007. "Displacement Amplification and Electric Characteristics of Modified

Rectangular Cymbal Transducers Using Electroactive Materials." *Solid State Communications* 143(6):321–5.

Maniccia, D., A. Tweed, A. Bierman, and B. Von Neida. 2001. "The Effects of Changing Occupancy Sensor Time-Out Setting on Energy Savings, Lamp Cycling and Maintenance Costs." *Journal of the Illuminating Engineering Society* 30(2):97–110.

Martin, P. E., and A. P. Marsh. 1992. "Step Length and Frequency Effects on Ground Reaction Forces During Walking." *Journal of Biomechanics* 25(10):1237–9.

Merron, J. 2004. "The NFL Weight Rankings." *Page 2*. Accessed April 24, 2014. http://sports.espn.go.com/espn/page2/story?page=merron/041124_rankings

Morales, M., and Z. Shivers. 2007. "Wireless Sensor Monitor Using the eZ430-RF2500": Texas Instruments.

Nguyen, T. A., and M. Aiello. 2013. "Energy Intelligent Buildings Based on User Activity: A Survey." *Energy and Buildings* 56:244–57.

Paulides, J., J. Jansen, L. Encica, E. Lomonova, and M. Smit. 2009. "Human-Powered Small-Scale Generation System for a Sustainable Dance Club". *Electric Machines and Drives Conference, 2009. IEMDC'09. IEEE International*.

Rees, D. W. 2009. *Mechanics of Optimal Structural Design: Minimum Weight Structures*. The Atrium, Southern Gate, Chichester, West Sussex, PO19 8SQ, United Kingdom: John Wiley & Sons.

Seow, Z. L., S. T. Chen, and N. B. Khairudin. 2011. "An Investigation Into Energy Generating Tiles: Pavegen." Accessed February 27, 2014. Retrieved from https://circle.ubc.ca/bitstream/handle/2429/43022/Seow_Z_et_al_SEEDS_2011.pdf?sequence=1

Sun, C. -L., S. Guo, W. Li, Z. Xing, G. Liu, and X. -Z. Zhao. 2005. "Displacement Amplification and Resonance Characteristics of the Cymbal Transducers." *Sensors and Actuators A: Physical* 121(1):213–20.

Texas Instruments. 2009. "eZ430-RF2500 Development Tool User's Guide." Accessed June 4th, 2014. http://www.ti.com/lit/ug/slau227e/slau227e.pdf

Von Neida, B., D. Manicria, and A. Tweed. 2001. "An Analysis of the Energy and Cost Savings Potential of Occupancy Sensors for Commercial Lighting Systems." *Journal of the Illuminating Engineering Society* 30(2):111–25.

Weng, T., and Y. Agarwal. 2012. "From Buildings to Smart Buildings—Sensing and Actuation to Improve Energy Efficiency." *IEEE Design & Test of Computers* 29(4):36–44.

Wilkie, W. K., R. G. Bryant, J. W. High, R. L. Fox, R. F. Hellbaum, J. Jalink Jr, … P. H. Mirick. 2000. "Low-cost Piezocomposite Actuator for Structural Control Applications." *SPIE's 7th Annual International Symposium on Smart Structures and Materials*.

Yan, Y., Y. U. Wang, and S. Priya. 2012. "Electromechanical Behavior of [001]-Textured Pb (Mg1/3nb2/3) O3-PbTiO3 Ceramics." *Applied Physics Letters* 100(19):192905.

Zhang, T.-Y., and C. Gao. 2004. "Fracture Behaviors of Piezoelectric Materials." *Theoretical and Applied Fracture Mechanics* 41(1):339–79.

Zhao, H., J. Yu, and J. Ling. 2010. "Finite Element Analysis of Cymbal Piezoelectric Transducers for Harvesting Energy from Asphalt Pavement." *Nippon seramikkusu kyokai gakujutsu ronbunshi* 118(10):909–15.